Development of macroporous silicon for bio-chemical sensing applications

Tiffany M. Hoover

Abstract—**Macroporous silicon bio-chemical sensing devices have been developed, fabricated and tested. The porous silicon walls were lined with oxide and aluminum electrodes were placed on either side of the porous silicon membrane. These electrodes were used to measure capacitive changes resulting from vapor/fluidic interactions with the oxide-coated porous silicon membrane.**

For thick flow-through membrane formation, the maximum etch time investigated during the porous silicon-forming anodization process, using an electrolyte consisting of hydrofluoric acid and dimethylformamide was an 8 hour period with an electrolyte refresh halfway through the process. The pore dimensions measured after this process were approximately 67μm at the center and 102um at the edge, with a pore width of 1.6μm to 1.65μm, respectively. The propagation was highly anisotropic with vertical pore sidewall profiles. Flow-through membrane structure devices were realized and electrical data was collected.

Index Terms—**anodization, bio-chemical detection, HF/DMF electrolyte, porous silicon, sensor**

I. Introduction

THOUGH research and literature on porous silicon is prevalent, the mechanisms which produce porous silicon, are not very well understood. A porous silicon bio-chemical sensor is a small device used to detect biological and chemical materials. The sensitivity of the porous silicon membranes to charged molecules and the large internal surface make this device a prime candidate for development [1].

The device can be placed in an environment to detect analytes in vapor and liquid phase. In the past, in order to carry out this kind of analysis, time is taken to extract the material, after which it is taken offsite and tested. This bio-chemical sensor is a much more efficient process. The sensor can detect the foreign material in minutes on a micro-contaminant level and it makes removal of the substance from the contaminated area unnecessary. This type of device can potentially be used in medical treatment for rapid diagnoses of patients brought into emergency care. Time and accuracy in detection can be vital to human life in many cases, so development is extremely useful [2].

For this specific device, the vapor in the environment travels through the macro-sized membranes of the device and attaches to the walls of the macroporous silicon lined with thermally grown oxide. The device can then detect the capacitive changes over time as the vapor saturates the pores, and potentially identify the substance based on the output characteristics. This device is a prime candidate for field effect sensing due to the increased surface area produced by the flow-through pore formation [1]. With research, the bio-chemical sensor can be integrated into detection systems for fluid/vapor sensing.

The goal of this project was to take a pre-existing macroporous sensor process, with the potential to become a full-scale bio-chemical sensor, and improve the porous silicon formation process for integration into fluidic/vapor detection systems. The result of this project should be a macroporous silicon device capable of detecting vapor, having the potential to detect liquid chemicals through capacitive characteristics. The process investigation should give insight into pore formation, diameter, and propagation depth of the membrane, as well as sidewall quality. This can be related to etching conditions such as current density, time and electrolyte refresh.

II. Theory

A. Macroporous Silicon

Porous silicon is silicon with a semi-random order of anisotropic pores formed through electrochemical etching. Porous silicon is classified into three categories based on pore diameter: (1) Micro-porous silicon with pore diameters and pore-to-pore distances smaller than 2nm~10nm; (2) Meso-porous silicon with pores in the 2nm~10nm to 50nm range; (3) Macroporous silicon with pores larger than 50nm [3], [4]. In this work the investigation focus is on macroporous silicon.

One method to form the porous silicon is through a process known as anodization or dissolution of silicon. In this process, a hydrofluoric acid (HF) solution is used to etch into silicon using anodic current densities. The anisotropic pore formation is due to dependence on the (100) crystallography orientation of the silicon surface and the resistivity of the substrates. A pure HF solution does not easily infiltrate pores during dissolution, due to wettability and capillary phenomena

This work is part of a capstone design requirement for a B.S. degree in Microelectronic Engineering at the Rochester Institute of Technology (RIT), Rochester, NY. The results of the project were first presented as part of the 23rd Annual Microelectronic Engineering Conference, May 2005 at the Rochester Institute of Technology. The manuscript was received on May 17th, 2005. This work was supported in part by a grant from the Infotonics Center of Excellence, awarded to the Microelectronic Engineering Department, Rochester Institute of Technology.

T. M. Hoover is with the Microelectronic Engineering Department, Rochester Institute of Technology, Rochester, New York 14623 USA

(uniformity issues), and thus adding a solvent is recommended. Adding Dimethylformamide (DMF), an organic solvent, to the electrolyte can enhance anisotropic etching by acting as a surfactant agent, allowing needed infiltration and better uniformity [1]. The end result is a pore diameter between 1-2um, depending on the applied current and ratio of HF to DMF.

The process by which anodization is carried out consists of a platinum electrode immersed in an aqueous solution of HF/DMF (Fig. 1). The electrolyte solution is placed inside a Teflon holder, such that only certain portions of the silicon substrate are in contact with the electrolyte whereas; other areas are masked off by an oxide/nitride protective layer.

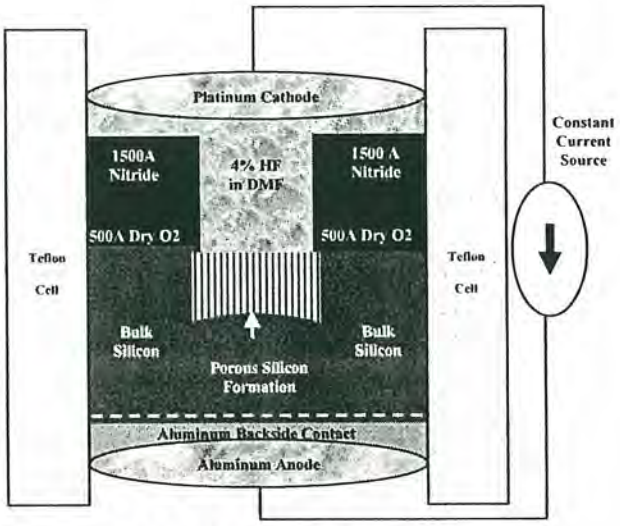

Fig. 1: Teflon Anodization Etching Cell

The backside of the substrate is protected from the electrolyte, and a layer of aluminum is sputtered onto the backside. The wafer backside is doped with p-type dopant, cured, and a drive-in process is performed previous to the sputtering, in order to improve electrical contact to the aluminum backside layer. A power supply is attached to the platinum electrode immersed in the electrolyte and to an aluminum puck in contact with the backside of the wafer. A positive voltage is applied between the wafer and the platinum electrode immersed in the HF/DMF solution.

However useful the anodization process is, trenches of porous silicon can only form so far into the silicon over a designated period of time. This is due to passivation effects where the density of the surface states is reduced as a function of time, thus increasing the stability of the silicon surface against further electrochemical attack [5].

Dissolution Reaction:

$Si + 2HF + \lambda h+ \rightarrow SiF2 + 2H + (2- \lambda) e-$

$SiF2 + 2HF \rightarrow SiF4 + H2$

$SiF4 + 2HF \rightarrow H2SiF6$

The chemical reaction within the anodization process takes place under bias conditions. The fluorine ions are drawn to the surface of the wafer, where the electron is transferred from the fluorine ion to the silicon. At the silicon surface, two fluorine ions bond with a silicon atom. The HF atoms in solution release the SiF4 molecule from the surface, leaving hydrogen atoms to bond with the underlying atoms. The SiF4 molecules, in solution, bond with HF molecules to form H2SiF6 [6].

A by-product of the chemical reaction is H_2 molecules, which form gas bubbles, and can potentially, adhere to the wafer surface. This could contribute to incomplete pore propagation and lead to non-uniformity. Otherwise, the H_2 molecules are released into the atmosphere through a vent hole in the Teflon cell apparatus [6].

Etching deep pores into the bulk of a substrate may take hours to complete. The extended process time to get deeper pores, results in non-uniformity at the pore propagation front. A possible cause for this non-uniformity could be that the silicon is depleted of carriers and holes are not available for the dissolution process. The outer pores propagate further due to more available holes in the surrounding bulk silicon, whereas the pores towards the center of the membrane only have holes from below the membrane, which is depleted of hole carriers [3].

B. KOH Etching (Potassium Hydroxide)

To form a free standing structure such that the pores propagate through the thickness of the wafer, a KOH process can be utilized. In this process, the remaining backside silicon thickness after anodization can be removed by immersing the substrate in 40% hot phosphoric acid (KOH) at 85C. This is done by placing the wafer inside a double-wafer apparatus, such that only the areas to be etched on the backside of the substrate are unprotected. If a device wafer is not available, a "dummy" wafer is required for the second slot in the KOH etching apparatus. This decreases the likelihood of fluid getting through one side of the apparatus and contaminating the device wafer. The KOH will fully etch away the remaining silicon from the unprotected backside regions in an angle formation of 54.3 degrees (Fig. 2) and establishes the suspended porous silicon flow-through membrane.

Fig. 2: KOH Etching Layout

In order to keep the KOH from penetrating the pores already formed during anodization, a protective layer, such as a nitride/oxide liner should be deposited into the pores. The high selectivity of silicon (~80um/hr) to nitride (<1nm/hr) and oxide (575nm/hr) will allow bulk silicon etching without damaging the pore formation [7]. After removal of the

oxide/nitride liner within the porous silicon, a flow through macroporous silicon membrane is realized.

III. PROCEDURE

Initially, twenty-five 4-inch (100) oriented boron-doped p-type silicon wafers with resistivity (rho) ~ 20-25 Ohm-cm were obtained. In order to fabricate the biosensor devices, the following process parameters were followed [8]. Wafers 7-21 were chemically mechanically planarized (CMP) on the backside, using the Strauss Baugh CMP tool, so that processing on both sides could be completed with a smooth surface (Fig. 3a). Levasil 50CK/30% slurry was used and the wafers were polished for ~22minutes/wafer and then cleaned with cleaning solution to remove any slurry particulate. All 25 wafers underwent RCA clean and 5000A of wet oxide was grown on wafers 1-21 (Fig. 3b) using recipe LFull 5000A. After this, wafers 1-21 were coated on the front side with Shipley 812 positive photoresist using the SVG wafer track and the backside oxide was etched off in 8:1 buffered oxide etch (BOE) for approximately 7.5 minutes (Fig. 3c).

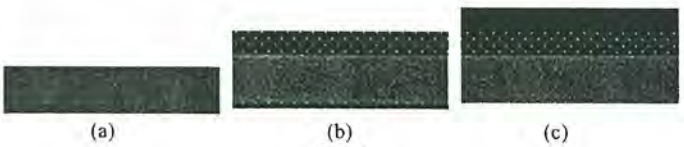

Fig. 3

The photoresist was then stripped using the Branson Asher (wafer # 21 broken) and the wafers were RCA cleaned before p-type Borofilm 100 dopant was spun onto the backside of wafers 1-20 (Fig. 4a). The dopant was driven in using the Bruce furnace and then a blanket 8:1 BOE wet etch of the 5000A wet oxide was completed (Fig. 4b) for ~15 minutes. After etch, 500A of dry oxide was grown in the Bruce 1 tube 4 furnace using recipe #458: SMFL 500A Dry Ox. Due to a transformer failure, the Dry Oxide had to be restarted as no film was deposited due to the failure. The deposition of nitride did not happen for a few weeks, as the tool had o-ring burn outs, leak check failures, and internal computer errors. When the LPCVD was finally back online, 1500A of nitride was deposited onto wafers 1-16 & 18-20 (Fig. 4c) using the 1500A SMFL Factory Nitride Recipe (Wafer #17 broken) with a deposit time of ~21 minutes.

Fig. 4

The device was then ready for the first anodization photolithography step. This step consisted of coating the wafers on the SVG wafer track, exposing the anodization area on the Karl Suss mask aligner for ~10 s, and developing on the wafer track (Fig. 5a). The nitride was then etched to open the anodization area on the front side using the LAM 490 FACNIT1500 Recipe. The backside was cleaned with acetone, and then placed back in the LAM 490 for backside nitride etch (Fig. 5b) using the same recipe. The oxide was then removed from the front anodization area, and the backside of the wafer, using 10:1 BOE for ~45 s. The resist was then stripped in the Branson Asher (Fig. 5c).

Fig. 5

Wafers 1-16 & 18-20 were RCA cleaned and dipped in 50:1 HF for 30s so that the sputtered Aluminum on the backside had a quality ohmic contact. After sputter, the wafers were sintered (Fig. 6a) using the SMFL Sinter 450C Recipe in Bruce 1, Tube 2. The wafers were then ready for their first major silicon wet etching step. A preliminary design was set up for the anodization process instead of a factorial design, due to the time required for each individual anodization process. Using an anodization Teflon cell apparatus seen in Fig. 1, wafers 1-3 were anodized in an electrolyte mixture of 4% Hydrofluoric Acid (HF) in Dimethylformamide (DMF). They were then cleaved and SEM imaged, as a test run for current density and process time values (Fig. 13). After approximations were established, wafers 4 & 7-12 were

anodized (Fig. 6b). Wafers 1-4, 7, 8, 11 & 12 were then cleaved and SEM images (see Fig. 15 - parameters) were taken. Wafers 9 & 10 were not cleaved and were sent on for device processing. The aluminum was stripped from 9 & 10 using aluminum wet etch for ~2 minutes at 50C followed by growing 1000A of dry oxide in Bruce 2, Tube 4 using Recipe #5: 100A SMFL Dry 02 (Fig. 6c).

(a) (b) (c)

Fig. 6

A 10:1 BOE deglaze (~30 s) was carried out to remove the oxy-nitride layer formed (Fig. 7a) from oxidization of the nitride. The nitride on the front side of the wafer was then etched with hot phosphoric acid for ~26 minutes at 175C. 1500A of SMFL stoichiometric nitride was grown in the LPCVD (Fig. 7b) using Recipe 1500A STO SMFL Nitride with a deposit time of ~75 minutes. At this point, the wafers were ready for their second major photolithography step; the KOH etch definition. The wafers were coated on the SVG wafer track with Shipley 812 positive photoresist, exposed for 10 s in areas to be KOH etched using the Karl Suss mask aligner, and then developed (Fig. 7c) on the SVG wafer track. Wafer #9 was broken during this processing step, so the front side was waxed to a dummy wafer to continue processing.

(a) (b) (c)

Fig. 7

The backside nitride was etched from both wafers using the LAM 490 FACNIT1500 Recipe and 9260 photoresist was painted onto the front side pores of wafer #10 to ensure protection. The backside oxide was then etched in 10:1 BOE for ~3.75 minutes and the 9260 photoresist and backside wax were removed (Fig. 8a) using an acetone overnight immersion soak. Wafer #9 was scrapped in order to save time due to process complications. Wafer #10 and a dummy wafer were sent through to KOH etching with a 40% solution in DI H_2O and a temperature of 85C (Fig. 8b). The wafer was checked at approximately 6 hours into the KOH etch time with a total etch time of 6.5 hours. After etch, the wafers were decontaminated to remove any potassium that can contaminate tools for MOS fabrication. This was done by immersing the wafers in a bath of self heating 1:1:1 DI H_2O: 30% Hydrogen Peroxide: Hydrochloric Acid for 20 minutes. Wafer #10 was dipped in 10:1 BOE, for a 30 second deglaze to remove any oxy-nitride film. The nitride was then stripped from wafer #10 in hot phosphoric acid at 175C for ~30 minutes. The pad oxide was etched off in BOE (Fig. 8c) for approximately 10 minutes to remove oxide lining the porous silicon membrane. At this point, the wafer was completely bare with only a flow-through porous silicon membrane.

(a) (b) (c)

Fig. 8

After making sure the wafer was completely bare by measuring for thickness on the Nanospec, 500A dry oxide was grown to re-oxidize the porous silicon membrane (Fig. 9a). Bruce 1, Tube 4 was used with the 500A Dry Oxide Recipe. The third photolithography step was used to define the contact cuts. Thick 813 photoresist was coated on the backside of wafer #10 and left to dry overnight. Then 9260 photoresist was spun on the front side of the wafer. The front side contact cuts were then exposed on the Karl Suss for 4 minutes 20 s, and developed (Fig. 9b) for 4 minutes 20 s using 4:1 DI Water:MF351 developer. The oxide was etched from the contact cut areas in 10:1 BOE wet etch for ~55 s and then the photoresist was stripped using acetone (Fig. 9c).

(a) (b) (c)

Fig. 9

To prepare wafer #10 for the aluminum contact deposition, it was RCA cleaned (NiSi contamination in the baths) and HF dipped for 15 s. 2um of aluminum was sputtered on the front side of wafer #10 (Fig. 10a). The final metal definition photolithography step served the purpose of protecting the contacts and etching away the remaining aluminum. This was done by coating the front side of wafer #10 with 9260 photoresist, exposing for 4 minutes 20 s on the Karl Suss, and developing (Fig. 10b) in 4:1 DI Water/MF351 for 4 minutes 20 s. The metal was then etched in aluminum wet etch for ~4 minutes at 50C and the photoresist was fully stripped using acetone. After N2 drying, a residue was found on the surface of the wafer. Wafer #10 was not sintered due to this contaminate issue (Fig. 10c). A broken wafer piece was tested in the Aluminum etch, to see if it was possibly un-etched aluminum, but this did not prove successful.

(a) (b) (c)

Fig. 10

At this point, wafer #10 was completely processed and ready for testing. A layout of the complete structure design

can be seen in Fig. 12. With the devices complete, the wafer was sent to test (Fig. 11). With an acceptable measured capacitance, the sinter step was not performed. The residue did not appear to hinder testing, so further testing commenced.

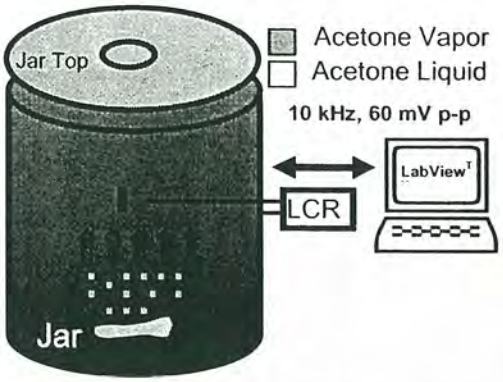

Fig. 11: Bio-Sensor Device Testing Apparatus

Top View - Layer Key:

(a) Top View

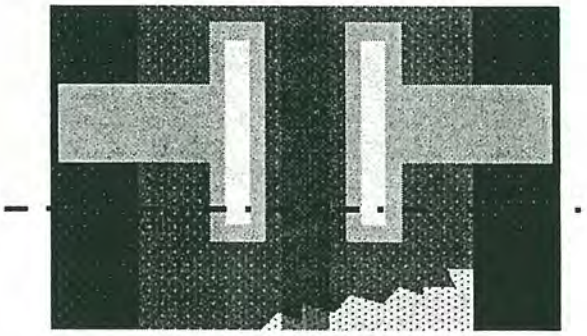

Side View - Layer Key:

(b) Side View

Fig. 12: Device Layout

IV. Results & Discussion

A. Anodization Data & SEM Imaging

The parameters in Fig. 13 (below) were used as a design of experiments for the anodization process. Wafers 1-3 were initially completed to set a basis for the current density, whereas 7, 8, 4, 11 and 12 were done as such for refresh experimentation and time. Wafers 9 and 10 were processed through to completed devices.

Wafer #	Current Density (mA/cm^2)	Constant Current (mA)	Time (hrs)	Refresh Time	Reverse Bias
1	4	8	4	2 hrs	0
2	6	12	4	2 hrs	0
3	2	4	4	none	0
7	4	8	8	4 hrs	0
8	4	8	6	3hrs+ 2hrs	0
9	4	8	6	3hrs+ 2hrs	0
10	4	8	6	3hrs + 2hrs	0
4 w/ 23 backside	4	8	6	3hrs+ 2hrs	0
11	4	8	6	3hrs+ 2hrs	1mA @ 3hrs/5hrs for 10mins 0.8mA @ 3hrs/5hrs for 18mins/12mins
12	4	8	6	3hrs+ 2hrs	

Fig. 13: Anodization Parameters

The results of SEM imaging of the anodized wafers can be seen below in Fig. 14. Each wafer was imaged for pore diameter, depth, and viewed for overall pore quality. As you can see, the diameters of all pores measured in this experiment are within the expected macroporous silicon range, being that they are larger than 50nm.

Wafer #	Pore Diameter	Center Pore Depth	Outer Pore Depth
1	1um-1.2um	50.56um	73.26um
2	1.5um-1.6um	34.90um	48.41um
3	2.2um-2.6um	12.03um	21.43um

7	1.61um	66.63um	102.4um
8	1.7um-2um	45.88um	68um
9	processed	--	--
10	processed	--	--
4 w/ 23 backside	2.117um-2.319um	20.72um	34.32um
11	1.889um-1.986um	59.00um	78.52um
12	1.350um-1.575um	44.25um	64.80um

Fig. 14: SEM Imaging Results based on anodization

A refresh did not occur for wafer #3 because the refresh did not help the pores form any faster. This was based on a comparison of the pore depth of wafer #1 and a wafer with the same parameters, processed by the research group, previous to this project (Fig. 15). Wafer #1 resulted in a center pore depth of 50.56um with a 2-hour refresh whereas the comparison wafer resulted in a center pore depth of 49.90um without refresh. As such, it was established that the refresh was only a waste of chemicals and time at the 2-hour point in processing.

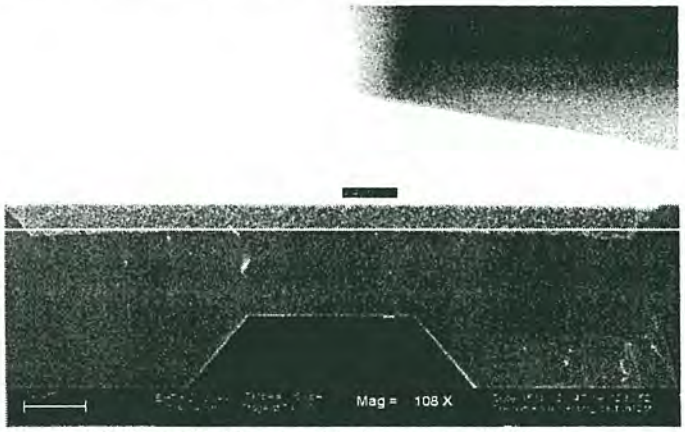

Fig. 15: wafer #1 comparison image (no refresh)

Each wafer, other than those designated as device wafers, was cleaved and cross-sections were imaged using the LEO SEM. The first experimental investigation looked at the pore diameter. As you can see in Fig. 16, an anodization process lasting 4 hours, with a current density of 4mA/cm^2 and a refresh at 2 hours, resulted in smooth pore propagation and the smallest pore diameters.

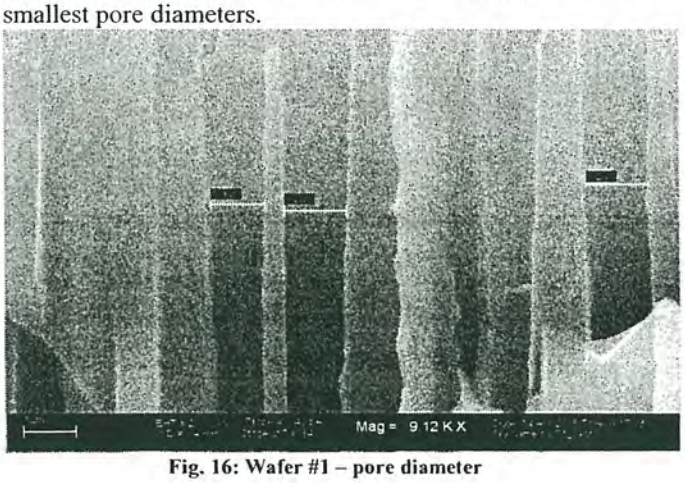

Fig. 16: Wafer #1 – pore diameter

In contrast to the pores formed during anodization of wafer #1, the image below in Fig. 17 shows what happened when the current density was decreased to 2mA/cm^2. The pores from this experiment were very shallow and the diameter was quite large, in reference to the other anodized wafers.

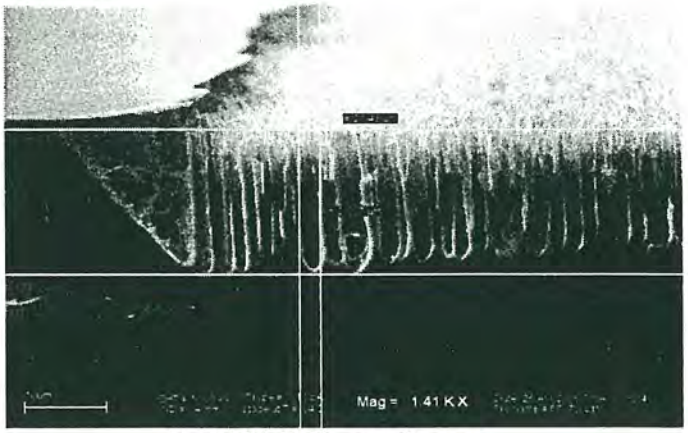

Fig. 17: Wafer #3 – pore diameter

Wafer #8, seen in Fig. 18, is also a very good example of the anisotropic nature of smooth pore formation, with a processing time of 6 hours (refresh at 3hrs, and 5 hours) and current density of 4mA/cm^2.

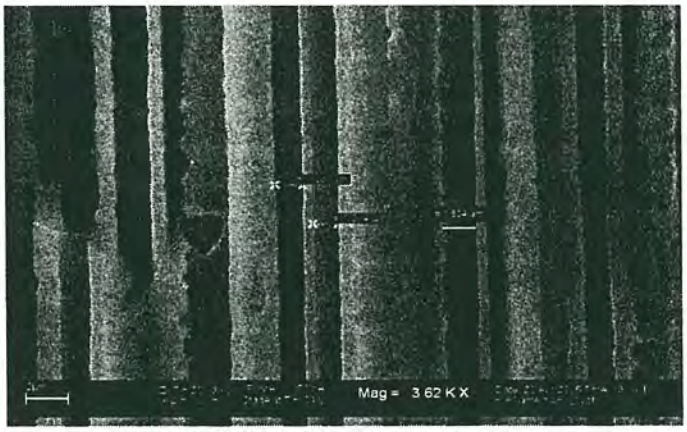

Fig. 18: Wafer#8 – pore diameter

The reverse biasing method [6] used for wafer #12 proved very rough on the pore propagation, as seen in Fig. 19. This could be attributed to loose hydrogen molecules being attracted to the porous silicon walls, thus coating them with by-product gas bubbles, and causing non-uniformity in pore sidewall formation.

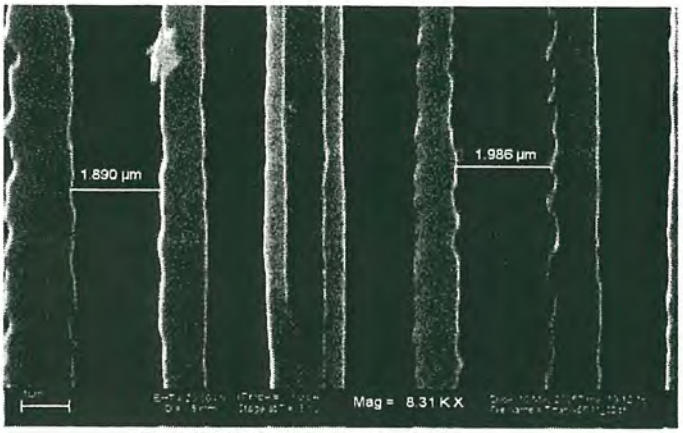

Fig. 19: Wafer#12 – pore diameter

The second experimental investigation was pore propagation depth. As you can see in the cross-section of wafer #7, Figures 20 & 21, the propagation depth was relatively uniform and propagation was maximized.

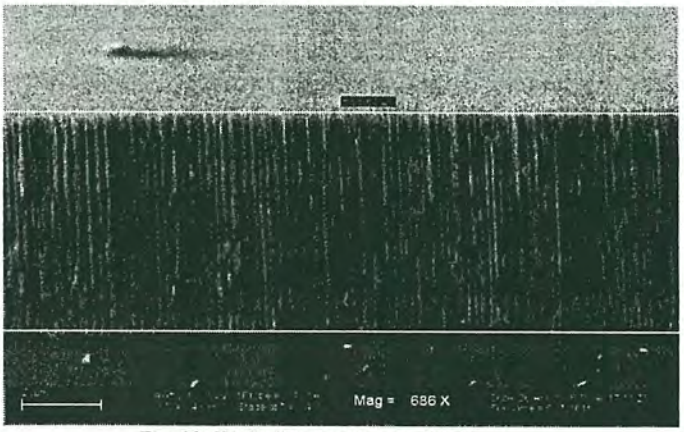

Fig. 20: Wafer#7 – inner pore depth

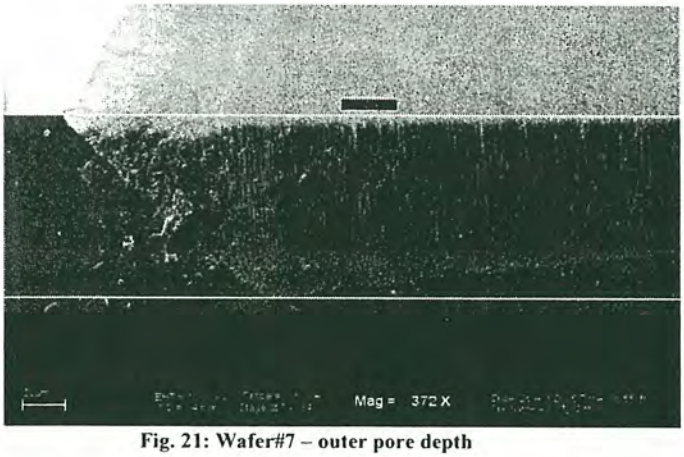

Fig. 21: Wafer#7 – outer pore depth

In contrast to this, wafer #3, discussed previously, and wafer #4 (Fig. 22) had the shallowest pore propagation depths. As stated, the current density and the backside wafer addition can be attributed to the causes. Wafer #4 had a second wafer applied to the backside, and there could have been contact problems between the two wafers, which caused the grass-like surface roughness formation and shallow depth.

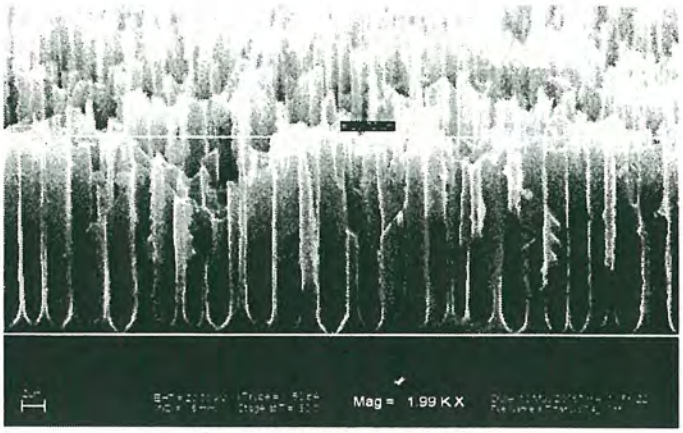

Fig. 22: Wafer#4 – pore depth

The addition of a bias to the anodization process did not give optimal pore quality, however the anisotropic propagation of the edge regions should be noted. Figures 17, and 21 can be compared to Fig. 23; the sidewall areas are rough and do not propagate horizontally. In the case of the reverse bias, the edge regions tend to propagate downward instead of sideways. This can potentially be attributed to the field effect being altered from the reverse bias, whereas the pores are given the chance to alter their course and revert to a horizontal propagation path.

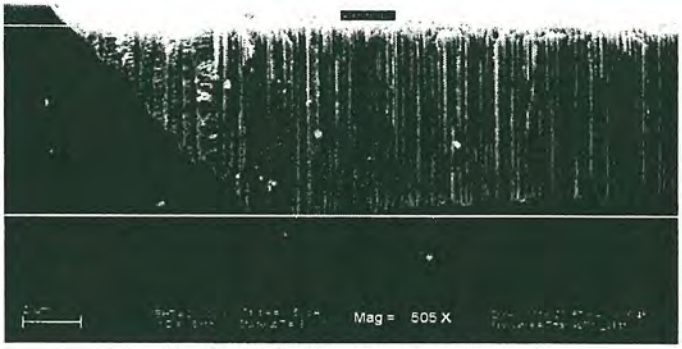

Fig. 23: Wafer#11 – outer pore depth

The current density was altered for certain wafers to see if the results gave a better pore propagation depth and pore diameter. In fact, the maximum current density used, resulted in a void along the edge of the porous silicon region, as you can see in Fig. 24. The results of the minimum current density were also not optimal, as discussed previously. Based on this, the median current density of $4mA/cm^2$ was kept throughout the remainder of the experiment. This value was previously used for anodization in past bio-chemical sensor fabrication.

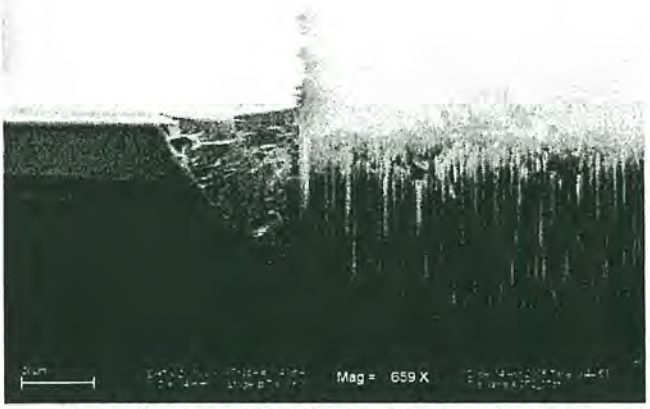

Fig. 24: Wafer#2 – Void defect due to high current density

B. Electrical Data

After processing, wafer #10 was taken to testing [8]. The initial capacitive test was for humidity, as you can see in the graph below (Fig. 25). The Lab View software began collecting capacitance values at a baseline for comparison. Then, standing a few inches from the device a person exhaled onto the device. The device was able to detect the localized humidity change. Over approximately 20 minutes, the moisture which condensed onto the sensor evaporated and the baseline capacitance was restored.

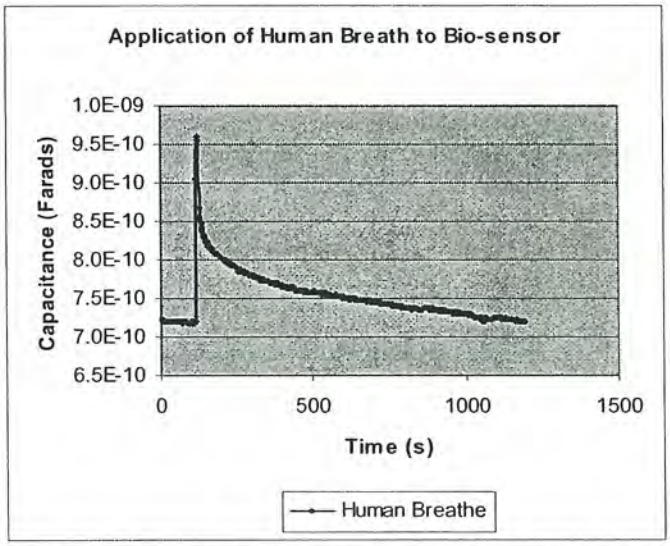

Fig. 25: Capacitive changes w/ application of human breath

The tests that followed were for acetone in vapor phase. The acetone vapor was exposed to the device to see how different concentrations affected the measured capacitance. Initially, the capacitance was base-lined and then 0.2mL of acetone was placed in the bottom of the testing apparatus (see Fig. 11). The device was left enclosed in the apparatus for approximately 6 hours, in order to fully vaporize the acetone and obtain capacitance data over time. The device was then left outside the apparatus for ~2 hours to remove any residual vapor. This test was then carried out for 0.7mL and then twice for 1.5mL, in the same manner. The baseline capacitance decreased for each consecutive experiment, so a possible solution to this would be allowing the device to sit in the atmosphere for a longer period of time.

As you can see on the graph in Fig. 26, the capacitance values for the 1.5mL vaporization dropped dramatically after a short period of time. This could be due to the epoxy that was used to attach the wires from the Lab view measurement apparatus to the aluminum contacts of the device. At this concentration, the acetone may chemically alter the epoxy causing a measured change in capacitance. A possible solution to this potential problem could be to not use epoxy at all. Rather, a viable solution could be contacting leads to the aluminum pads through a clamping mechanism.

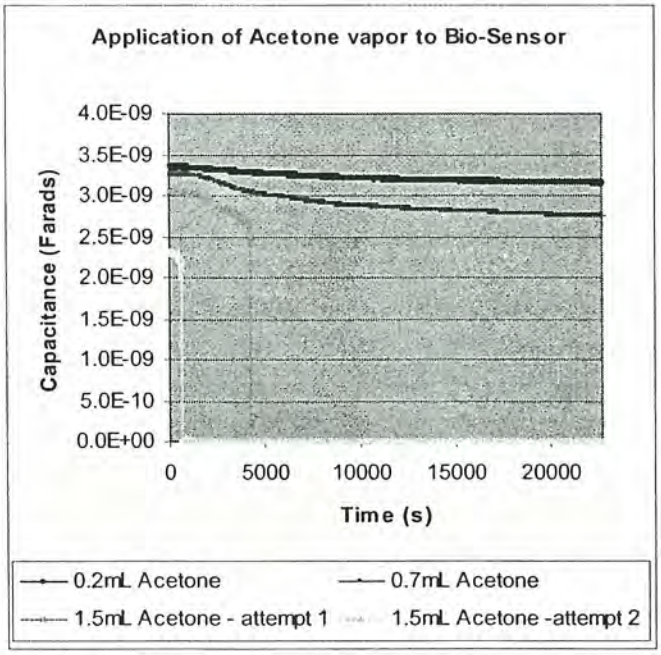

Fig. 26: Capacitive changes w/ application of acetone vapor

V. Conclusion

Investigation of porous silicon formation at the Rochester Institute of Technology has been completed. This work has resulted in better understanding of macroporous silicon material for fabrication of free standing macroporous silicon membranes in bio-chemical sensing applications. The maximum pore depth was achieved in 8 hours (4 hour refresh) with a current density of 4mA/cm^2 in an electrolyte consisting of 4% HF in DMF.

The engineered porous silicon films were then implemented for complete fabrication of bio-chemical sensors. Electrical tests consisting of relative humidity and solvent detection were conducted to demonstrate that the newly developed porous silicon material could be successfully integrated for fabrication of sensors.

The newly fabricated devices successfully detected humidity and solvents. During the testing, a unique decrease in capacitance was found during detection of high levels of acetone vapor. For the future, a possible solution would be to

try using metal wiring that does not require conductive epoxy. It is hypothesized that the epoxy, when chemically altered, suddenly causes a decrease in the measured capacitance.

ACKNOWLEDGMENTS

The author would like to thank Dr. Sean Rommel for his advising and guidance in the presented work; Also, Dr. Karl D. Hirschman, of the Rochester Institute of Technology for his advising and overall support in the macroporous silicon bio-chemical sensor project. She would like to thank Jeff Clarkson, a graduate student in the Microelectronic Engineering department, for his persistence and dedication to her success, willingness to always be there to answer questions and for always providing support when it was needed most. Other individuals the author would like to thank include graduate/undergraduate students Stephen Sudirgo, Mike Latham, Pat Warner, Dan Jaeger, and Dave Pawlik, among others, for working as a team to help get projects done on time; Also, The SMFL staff members for keeping the fab running smoothly throughout the quarter.

REFERENCES

[6] M. Archer, D. Persaud, K. D. Hirschman, M. Christophersen and P.M. Fauchet, *Electrical porous silicon microarray for DNA hybridization detection*, Mat. Res. Soc. Symposium Proceedings, 782, (2004) A7.2.

[7] Mathew, F. P., Alocilja, E. C., *Fabrication of porous silicon-based biosensor*, Sensors, 2003. Proceedings of IEEE, Volume: 1, Oct. 22-24, 2003, Pages: 293 – 298.

[8] Lehmann, V ., *Porous silicon - a new material for MEMS*, Micro Electro Mechanical Systems, 1996, MEMS '96, Proceedings. 'An Investigation of Micro Structures, Sensors, Actuators, Machines and Systems,' IEEE, The Ninth Annual International Workshop on, 11-15 Feb. 1996, Pages: 1 – 6.

[9] Huimin Ouyang, Lisa A. DeLouise, *Biosensing with one dimensional photonic band gap structure*, RIT, University of Rochester, 2004.

[10] Claussen, J.C.; Carstensen, J.; Christophersen, M.; Langa, S.; Foll, H., *Open-loop-control of pore formation in semiconductor etching*, Physics and Control, 2003. Proceedings, 2003 International Conference, Volume: 3, 20-22 Aug. 2003, Pages: 895 - 900 (vol. 3).

[11] James Seefeldt, Yogesh Gianchandani, *A porous silicon process for encapsulated single crystal, surface micromachined microstructures*, SPIE Conference on Micromachining and Microfabrication Process Technology, Volume: 3874, September 1999.

[12] J. Electrochem. Soc. Vol 137, 11, Nov 1990, 3612-3632; Available: http://www.ee.byu.edu/cleanroom/KOH.phtml

[13] Karl D. Hirschman, M. Archer, *Integrated sensor arrays with a configurable network interface for chemical and biological detection*, RIT, University of Rochester, 2004.

Tiffany M. Hoover, originally from Rochester, NY, received a B.S. degree in microelectronic engineering in May 2005, from the Rochester Institute of Technology in Rochester, NY. She completed her senior project requirement by studying porous silicon as it relates to bio-chemical electrical sensing.

She began her co-operative education as a Student Engineer in Winter 2001, at RIT, for a joint venture between Rochester Photonics Corporation and the Department of Microelectronic Engineering, where she worked with KOH etching techniques, wafer bonding and assisted in the instruction of a freshman seminar class. In Spring 2002, she continued working at RIT as a Student Engineer for the Laboratory for Cooperative Microsystems (LYCOMS), where she assisted in the development of micro shutters and micro coils, advancement of carbon nanotube technology and worked with deep silicon trench etching equipment. She joined Micron Technologies in Manassas, Virginia during Spring/Summer of 2003 as a PECVD Intern Engineer in the plasma enhanced chemical vapor deposition department. In the Winter of 2004, she worked for the University of Rochester Laboratory for Laser Energetics in Rochester, NY, as a Student Intern Engineer, developing wet chemical etching techniques for the OMEGA EP laser diffraction gratings and continued research on SU-8 photolithography processing of liquid crystal point diffraction interferometry devices. Currently, she is still working part-time for the University of Rochester Laboratory for Laser Energetics in both wet etching and photolithography.

Miss Hoover has been very active in the academic community throughout her undergraduate career. She began her college career as a National Action Council for Minorities in Engineering (NACME) Vanguard Scholar, winning a full scholarship to RIT, where she continued her participation as a group member. She actively participated in the Society of Women Engineers as a member, vice president and president, where she attended the Society of Women Engineers 2001 Nationals in Denver, Colorado. She also actively participated in the Microelectronic Engineering Student Association (MESA) as a member, vice president and president, where she helped establish the senior design award.